

Real and reactive power control of distributed PV inverters for overvoltage prevention and increased renewable generation hosting capacity



L. Collins ^{a, b}, J.K. Ward ^{a, *}

^a CSIRO Energy Technology Centre, 10 Murray Dwyer Circuit, Mayfield West, NSW 2304, Australia

^b University of Newcastle, University Drive, Callaghan, NSW 2308, Australia

ARTICLE INFO

Article history:

Received 18 February 2014

Accepted 7 March 2015

Available online

Keywords:

Reactive power

Active power curtailment

Photovoltaic inverter

Distributed generation

VAR control

ABSTRACT

Australia has seen a strong uptake of residential PV systems over the last five years, with small scale distributed generation systems now accounting for around 10% of peak capacity within the Australian National Electricity Market. As uptake further increases, there is concern about the ability of distribution networks to maintain reliability and power quality without requiring substantial additional infrastructure investment, and in some locations PV installations are no longer being allowed.

This paper evaluates the effectiveness of real and reactive power control of distributed PV inverter systems, to maintain and improve network power quality. High resolution PV output data has been collected at a number of trial sites in Newcastle, Australia and network impact simulations undertaken for an example long rural feeder gathered from the Australian National Feeder Taxonomy Study. These show how localised PV inverter controls can regulate distribution network voltages, reduce network losses, increase the network hosting capacity and hence the uptake of distributed renewable energy.

© 2015 Elsevier Ltd. All rights reserved.

1. Introduction

Australia's energy sector is in the midst of a fundamental transformation. On the generation side, renewable energy is expected to provide 20% of Australia's electricity needs by 2020 and low emissions technologies are expected to have replaced almost all conventional generation by 2050. Energy usage patterns are also changing, particularly with the widespread uptake of residential air-conditioning – which has driven growth in peak demand relative to energy consumption and consequently undermined existing energy based revenue structures.

Responding to changing energy usage patterns and the intermittency of renewable (particularly PV) generation, means transitioning the electricity network from a one-way bulk transport system, to a transactional system with controllable generation and loads throughout. Fortunately, there are a number of technology

and market changes taking place that combine to make this a realisable, if ambitious goal:

- Community awareness and engagement in the management of the electricity system is increasing, partly due to considerable pricing increases;
- Off-grid and local generation systems are becoming viable in their own right – PV module prices have plummeted and battery and balance of system costs have been steadily dropping;
- The technologies for consumers to participate in demand management are maturing – HAN (Home Area Network) controllers are now being included in smart meters, while standards are becoming available for appliance demand and inverter advanced power quality responses;
- Smart meters that not only measure consumer energy usage, but also network conditions, have been extensively trialled and are suited to main-stream deployment;
- New sensing technologies allow for easier monitoring of HV (high voltage) transmission systems, giving a clearer picture of network conditions and behaviour;

* Corresponding author. CSIRO Energy Technology, PO Box 330, Newcastle 2300, Australia. Tel.: +61 2 49606072.

E-mail addresses: Lyle.Collins@csiro.au (L. Collins), John.K.Ward@csiro.au (J.K. Ward).

- Data storage capabilities and communications speeds have increased substantially, making it possible to measure and store better information than ever before; and
- Algorithms are being developed to manage 'big data', providing network control system optimisation and taking advantage of improvements in communications and computational power to rigorously evaluate alternate control scenarios before committing to a particular action.

The challenge is to now build the social, technical and regulatory systems to support this transformation. One aspect of this, and the focus of this paper, is the technical challenge of increasing the PV hosting capacity of distribution networks. With PV installations in Australia now nearing 10% of the peak capacity of the National Electricity Market (NEM), concern over the potential impacts that this may have, has led some electricity companies to begin restricting PV installations in particular geographical areas. Such restrictions have been attributed to concerns over power quality, specifically voltage rise problems ([1], pg. 75). The voltage rise problem is well established as occurring, though its significance in determining limits of PV adoption is not.

To help make this assessment, high resolution PV output data and network voltages have been collected at a number of trial sites in Newcastle, Australia and network impact simulations undertaken for an example feeder from the Australian National Feeder Taxonomy Study (NFTS). The NFTS was conducted by the CSIRO as part of the Ausgrid Smart Grid Smart City trial (see www.smartgridsmartcity.com.au), with input from electricity distribution companies from across Australia, and has created a classification of feeder types in Australia and a representative set of example feeders. A similar study of US feeders was undertaken by the PNNL (Pacific Northwest National Laboratory) [2]. The NFTS allows the applicability of experimental results on a particular feeder to be understood in terms of their significance across Australia and hence build the business case for specific network management and control approaches.

This paper compares and reports the effectiveness, using experimentally obtained data in combination with network simulations, of a variety of inverter control strategies to reduce voltage rise. Several of these strategies are described in the Electric Power Research Institute's report on smart inverter functions [3], however additional control features are also tested, specifically with the aim of evaluating the appropriateness of the schemes for upcoming revisions to Australian Standards AS/NZ4755 and AS/NZ4777.

Although different inverter manufacturers have adopted different approaches for when network power quality problems are detected, one standard function is for inverters to shut-off on detection of over-voltage conditions, resulting in the 100% loss of power generation (and thus earnings) for the PV owner for the duration of the event (which is often at peak tariff times). Another common voltage rise mitigation strategy is to curtail active power (the APC – active power curtailment – strategy), which is explored in Refs. [4,5] which produces beneficial results. An example of this behaviour is shown in Fig. 1 (which also shows curtailment behaviour when PV power is below a minimum level). However, by using knowledge of the electricity network and loads – that loads and network lines are typically inductive – a more intelligent control scheme for inverters can be implemented that utilises reactive power control to reduce the amount of real power curtailed, while providing a greater reduction in overvoltage. This type of control strategy is explored in Refs. [6,7], with profit-generating motives in Ref. [8], and with a more sophisticated controller in Ref. [9]. While these and many other papers propose and evaluate alternative schemes, this paper is instead focused on comparing the

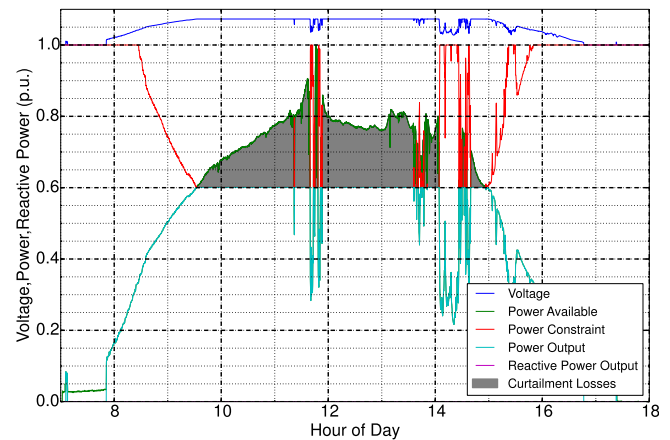


Fig. 1. Example of over-voltage curtailment.

relative performance, specifically considering curtailment losses, of different types of inverter control models.

The feeder used for these simulation studies is from the Australian NFTS, though it has been anonymised and simplified for use in this paper. The simulation results are therefore useful for comparing the different inverter control schemes, but would need to be tested across the range of prototypical feeders before an assessment could be made of the PV hosting capacity of the existing Australian electricity system or existing PV curtailment losses therein. This will be a subject of our future work. Of final note is that in this paper, *penetration* refers to the proportion of the peak load power that is provided by the PV at the peak generation time.

2. Experimental platform

PV generation data, together with customer load and voltage measurements were collected from a number of trial sites in Newcastle, Australia. This experimental platform was setup to support the CSIRO Virtual Power Station (VPS), which aggregates a large number of geographically dispersed and technically diverse small scale renewable energy generators together to form a 'virtual power station', which presents to the electricity system as a single reliable dispatchable entity. This dispatch capability can be used to manage exposure to high NEM spot prices or to address specific network constraints by exporting additional (stored) energy when required.

For the VPS trial, each of the 20 individual site nodes were retrofitted with a small embedded controller (see Fig. 2) that interfaces to the inverter to monitor energy which is communicated to the VPS central control and monitoring system hosted by CSIRO. Site PV sizes ranged from 1 kW to 10 kW, with the total trial VPS system peak output just over 50 kW. Sites that have both generation and battery storage also receive a battery charge setpoint from the VPS central control system, which is used to balance the total output of the VPS as is required due to the inevitable (minor) mismatch between forecast and actual generation output. The planned VPS output is determined on a 5 min cycle (consistent with the Australian National Energy Market dispatch cycle) and regulated with a 10 s control loop. Communications between sites is achieved using 3G wireless modems, which operate to transfer data over the existing mobile phone network.

The VPS central control system also implements a database storing 10 s sampled data from each of the sites and provides a web interface. This allowed easy visualisation and reporting of the system performance, and has also served as an engagement tool for



Fig. 2. Example of a VPS node, consisting of a SMA inverter connected to an embedded controller with wifi communications.

trial participants, allowing them to monitor their systems in real time, in comparison to other sites, and see their contribution to the VPS system as a whole. This database now has over 1 year of high resolution PV, voltage and load data for each of the trial sites and provided a base data-set for the simulations detailed in this paper.

3. Voltage-rise mitigation strategies

Voltage rise due to PV generation within distribution networks is currently a key factor limiting deployment of distributed renewable energy systems. We now describe several types of voltage-rise mitigation strategies, before evaluating their effectiveness on example network scenarios. In describing the behaviour of each inverter, we adopt the following nomenclature:

- P_{avail} the available real power (W);
- P_{max} the desired real power operating point (W);
- P_{out} the real power output (W), +ve is export to the grid;
- Q_{inj} the reactive power operating point (VAR), +ve is inductive;
- Q_{op} the desired reactive power operating point (VAR);
- S_{rated} the apparent power rating (VA).

3.1. Active power curtailment (APC)

The simplest of mitigation strategies is the active power curtailment (volt–watt) strategy. In this case, the maximum permitted power exported by an inverter is limited to P_{max} , defined by corner points (V_1, P_1) and (V_2, P_2) as:

$$P_{max} = \begin{cases} P_1 & ; V < V_1 \\ P_1 - \frac{(V - V_1)(P_1 - P_2)}{(V_2 - V_1)} & ; V \in [V_1, V_2] \\ P_2 & ; V > V_2 \end{cases} \quad (1)$$

The actual operating point of the inverter will then be further constrained by the actual available power (limited by the available solar resource in the case of PV), giving:

$$P_{out} \leq P_{APC} = \min(P_{max}, P_{avail}) \quad (2)$$

The constraint/curtailment curve, along with the specific values used in this report, is shown in Fig. 3. If the voltage seen by the inverter (in this case, considered to be at the point of common

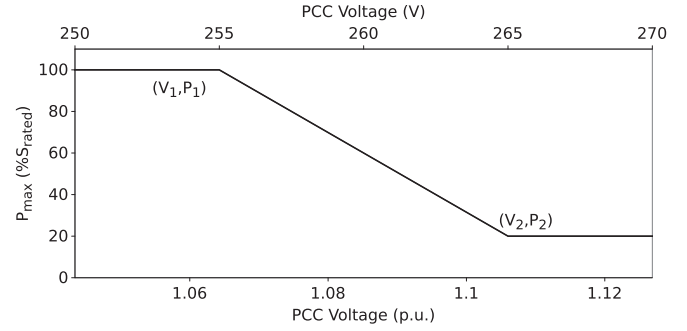


Fig. 3. The volt–watt function.

coupling (PCC)) increases beyond a specified limit, the inverter adjusts operation of the maximum power point tracker to reduce output power – effectively spilling power and generating less than it could for the available solar irradiance. All of the control models simulated in this paper that provide reactive power control also include APC, and are compared to a base control model that only has APC. Note also that the modelled inverter will disconnect if Watt production from the photovoltaics is less than $0.05S_{rated}$, where S_{rated} is the VA rating of the inverter.

3.2. Reactive power injection and absorption

In addition to APC, the volt–var function (seen in Fig. 4 showing the specific values used in this report) is used in conjunction with the Volt–Watt function (i.e. both control functions are active) to further manage network voltages via reactive power injection or absorption.

The desired reactive power absorbed by the inverter (Q_{op}), is defined by corner points (V_1, Q_1) , (V_2, Q_2) , (V_3, Q_3) and (V_4, Q_4) as:

$$Q_{op} = \begin{cases} Q_1; & V < V_1 \\ Q_1 + \frac{(V - V_1)(Q_2 - Q_1)}{(V_2 - V_1)}; & V \in [V_1, V_2] \\ Q_2 + \frac{(V - V_2)(Q_3 - Q_2)}{(V_3 - V_2)}; & V \in [V_2, V_3] \\ Q_3 + \frac{(V - V_3)(Q_4 - Q_3)}{(V_4 - V_3)}; & V \in [V_3, V_4] \\ Q_4; & V > V_4 \end{cases} \quad (3)$$

Note that these V_1 to V_4 are potentially different to those voltages for the APC.

Unlike the Volt–Watt function, the volt–var function should not be interpreted as a constraint curve. Instead, it should be interpreted as the ‘desired reactive power operating point’ (Q_{op}). The

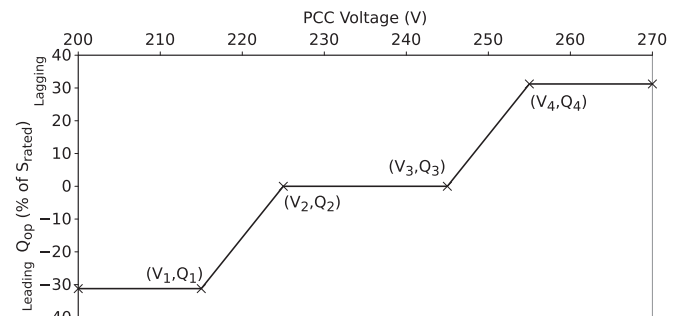


Fig. 4. The volt–var function.

specific values used in defining the volt–var function can be chosen so as to inherently create a degree of equity amongst the inverters. This can reduce the likelihood of any single inverter having to operate at $S = S_{rated}$ for any significant period of time due to over-voltage. In this way, the ‘burden’ of reducing extreme over-voltage can be largely shared amongst the inverters within the network segment suffering from over-voltage, and in proportion to their individual rated apparent power (S_{rated}). For example, see Ref. [10].

Both the desired real and reactive power operating points may not be able to be achieved simultaneously, being limited by the rated apparent power of the inverter. Specifically, the real power output (P_{out}) and reactive power (Q_{inj}) must satisfy Equation (4) where S_{rated} is the maximum apparent power that the inverter is capable of delivering (and may further be dependent on temperature and other operating variables).

$$P_{out}^2 + Q_{inj}^2 \leq S_{rated}^2 \quad (4)$$

There are three basic responses to this limitation:

Real power preferred – where real power is set according to equation (2), and reactive power is then determined to minimise $|Q_{inj} - Q_{op}|$ subject to equation (4);

Reactive power preferred – where reactive power is set equal to Q_{op} according to equation (3), and real power is then determined to maximise $|P_{out}|$ subject to satisfying both equations (2) and (4);

Constant power factor – where $P_{out} = \alpha P_{max}$ and $Q_{inj} = \alpha Q_{op}$ for α maximised subject to both equations (2) and (4).

Note that for the majority of the time, photovoltaic systems operate at well below their peak ratings so the resultant behaviour of the different control approaches usually will not differ significantly. For the simulations described in this paper, where we have limited $|Q_{inj}|$ to $0.31 \cdot S_{rated}$ (corresponding to a power factor of 0.95 at rated apparent power), the differences seen in simulations have been minimal, so we have chosen to mostly focus on the *reactive power preferred* control performance in the presented results. This would not be case where substantially larger amounts of reactive power are used, or where stronger solar resources mean that the inverter operates closer to the maximum ratings for a much greater proportion of the time.

3.3. Dynamic reference setpoint

There are a further two subcategories of control models simulated in this study – *static maximum* (SM) reference and *dynamic maximum* (DM) reference. For the case of a SM reference, active power curtailment is limited with respect to the rated inverter (apparent) power (S_{rated}) and is not dependent on current output power levels. The voltage-rise mitigation strategies described earlier in this section are of the SM type.

For the DM reference type model, real-power curtailment occurs relative to the inverter operating point at the time that the over-voltage conditions occur. Specifically,

$$\tilde{P}_{max} = P_{max} \cdot \bar{P}_{out} / S_{rated} \quad (5)$$

where \tilde{P}_{max} is the DM power constraint, P_{max} is per equation (1), and \bar{P}_{out} is the average real power over an interval immediately prior to the over-voltage condition occurring (in our simulation studies, this is the instantaneous power prior to curtailment). The actual output power is then limited, similarly to equation (2). The DM scaling factor ($\tilde{P}_{out} / S_{rated}$) is reset once the voltage returns to normal regulation conditions (less than V_1 in Fig. 3).

As an example of the DM curtailment strategy, consider two over-voltage scenarios – firstly where the inverter has been

operating at full rated power ($P_{out} = S_{rated}$) and secondly where the inverter has been operating at half rated power ($P_{out} = 0.5 \cdot S_{rated}$). At the time t_0 when over-voltage occurs ($V \geq V_1$ in Fig. 3), the DM scaling factor is calculated and real-power constraints are enacted as shown in Fig. 5 for the two scenarios. Note that in the special case where the DM scaling factor is 1, the SM and DM schemes are identical.

This real power constraint curve is then in effect until voltage returns to within regulation conditions, at which point the DM scaling factor is discarded and will be re-calculated next time an over-voltage condition occurs. The attraction of the DM type response is that real-power curtailment begins immediately once the threshold voltage is exceeded, providing a more immediate response and better regulation of network voltage. This also means, by extension, that more real-power is curtailed. This will be explored in simulation in the next section.

4. Simulation design

4.1. Small example model

An example of a small 3-node, 3-phase LV (low voltage) network is shown in Fig. 6. This model will be used to demonstrate the operation of the over-voltage mitigation schemes presented in the previous section, and their relative impacts on the performance of a distribution network. The network features a 415 V line to line delta-connected voltage source, connected to the remainder of the network through a star-connected 1 km overhead line (*GridConnect*) which has a total impedance of $1.5\Omega + 0.5j\Omega$ (PI modelled). The neutral of the *GridConnect* line is connected to ground at the voltage source end. The other distribution line (*Line*) is identical in all of its parameters (i.e. length, resistance and inductance). Each of the loads is modelled as having a peak power consumption of 5 kW, and operates with a constant 0.95 lagging power factor, though the power output varies throughout the simulated day according to a statistically generated profile (this is described in the following section). Both of the photovoltaic systems have a statistically generated solar power profile and a rated apparent power of 10.5 kVA, chosen as twice the maximum apparent power of the simulated loads. This very high penetration level was chosen to better demonstrate the effect of the controllers in reducing over-voltage.

The simulated performance of this system, demonstrating the difference between a SM *real power preferred* model against a SM APC only model are shown in Fig. 7. In the figure, the ΔV and ΔP refer to the voltage and power exported at the terminal of *PV_Terminal1* for a APC only model subtracted from a SM *real power preferred* model. In the figure, the i_q curve refers to the quadrature current (the photovoltaic units are modelled as current sources),

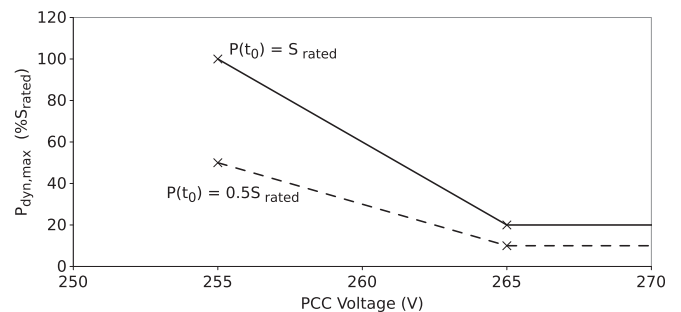


Fig. 5. Outline of the dynamic maximum type control model.

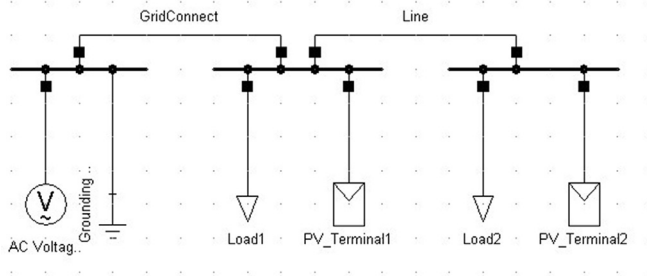


Fig. 6. Small LV Example network.

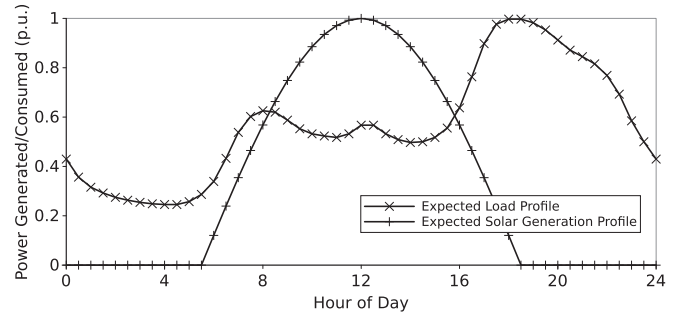


Fig. 9. Load and generation profiles forming the basis of the statistical profile generation.

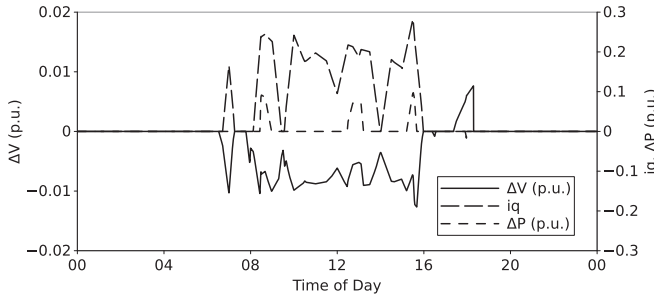


Fig. 7. Small example model simulation results.

and indicates when reactive power is being injected/absorbed by *PV_Terminal1*.

For this example system, we see that throughout the middle of the day, the SM, Real pref. model reduces overvoltage by around 1% with the use of quadrature current, via the volt–var function. Furthermore, there are specific times, particularly during peaks in PV power production where the SM *real power preferred* model is able to simultaneously reduce the over-voltage and increase real power exported (by around 10%). One other aspect of this simulation worth noting is the increase in voltage at approximately 18:00. This is due to the reactive power support provided by *PV_Terminal2* for under-voltage conditions, which occurs in this scenario because of a relatively large *Load1* & *Load2*. *PV_Terminal1* did not contribute to the reactive power support at this time as the inverter was shut down as the simulated solar resource was below the minimum threshold (0.05 per unit).

4.2. Simulation scenario – MV long rural

The small example system in the preceding section was used to demonstrate the basic behaviour of the volt–var and volt–watt power quality functions. We now describe a more realistic simulation scenario, namely a 33 node network with 11 loads on a MV (medium voltage) long rural network as shown in Fig. 8. This long rural feeder is an example of that gathered from the Australian National Feeder Taxonomy Study.

As the feeder operates at MV, loads in the network are attached to transformers, which step the voltage down to the low voltage

typical for residential customers – thus there are no LV distribution lines in this model. The performance metric we consider is the average voltage, calculated from the voltage at each node, which are nominally 11 kV. To simulate a weak grid connection, as is known to be common on such rural feeders, the external grid voltage was modelled as 15 kV, with a series resistance of 2 Ω, providing overvoltage conditions ($V \geq 1.06$ p.u.) and a reasonable voltage spread as a function of time. Transformers were considered to have fixed turn ratios (no automatic tap-changing) and network lines were modelled using lumped parameters. Although the properties of this weak grid connection were assigned somewhat arbitrarily to allow testing of the different inverter control schemes under substantial voltage fluctuations, this does not undermine the core findings of this paper on the relative benefits of the different inverter voltage control schemes.

In order to simulate high penetrations of embedded renewable energy, at each of the (11) nodes with the pre-existing loads, static generators (i.e. PV generators) were added to the simulation model. The rated apparent power of each of the generators was chosen to be equal to the peak real power consumption of the corresponding load. Each of the loads and generators were then given a statistically generated load profile (based on those in Ref. [11]) and PV generation profile respectively. The statistical PV generation profile was based on the profiles presented in Fig. 9 forming the expected value (at 30 min timesteps) for a β probability distribution with $\alpha = 2$ and $\alpha = 1.5$ for the load and solar generation profiles respectively. The specific realisation of these statistically generated profiles is maintained between simulation runs to allow comparison of results. The purpose behind statistically generating the load and solar profiles was to simulate approximately the effects of cloud cover and load variation. Load and PV generation data from the VPS was used to validate the characteristics of these simulated profiles. Figs. 10 and 11 show the comparison between the beta distribution function and measured data for both the solar and load profiles.

Simulations were performed with DigSILENT PowerFactory using the Newton–Raphson algorithm.

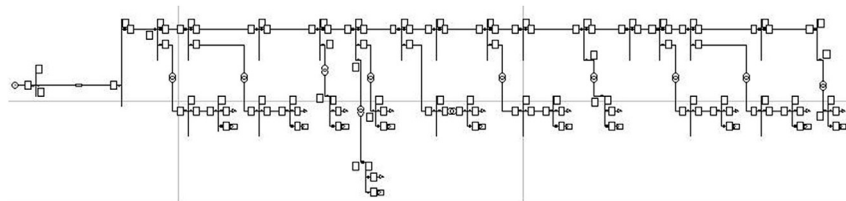


Fig. 8. MV long rural demonstration network.

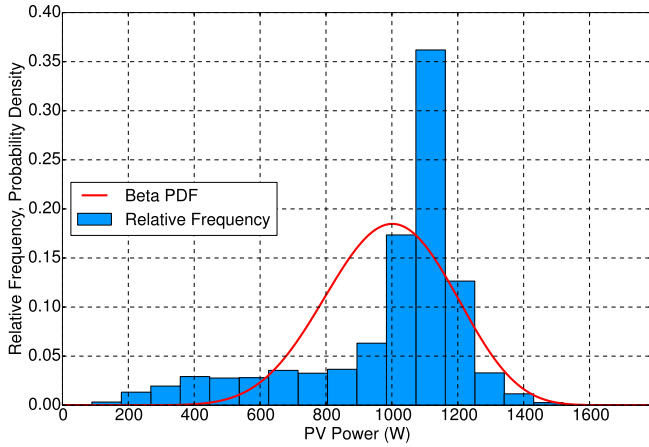


Fig. 10. Solar data collected from a VPS site approximated using the beta probability function.

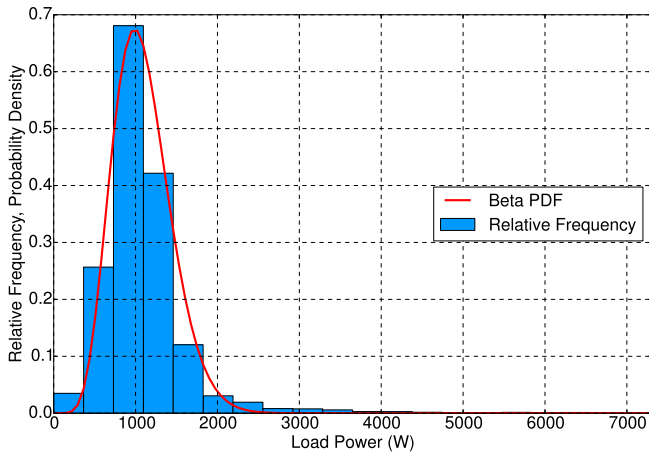


Fig. 11. Load data collected from a VPS site approximated using the beta probability function.

5. Simulation results – MV long rural

Using the MV long rural example system, initial simulations were carried out for varying levels of PV penetration without any voltage mitigation control active. Simulation results are shown in Fig. 12 and it is the 100% penetration scenario that will be used as a base case in the further analysis.

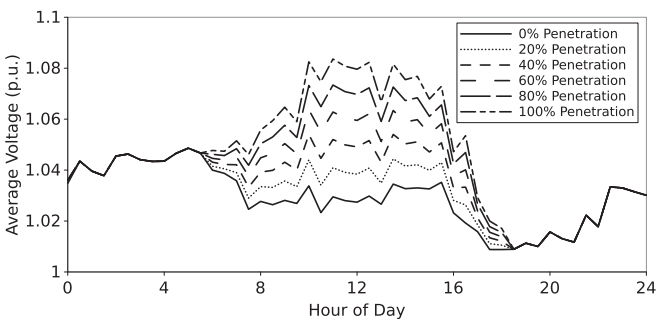


Fig. 12. The effects on average network voltage of increasing the photovoltaic penetration.

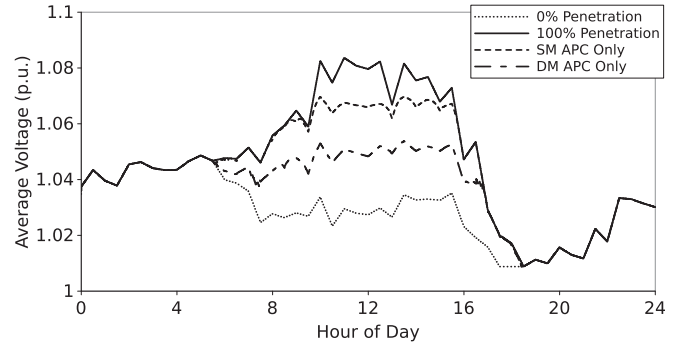


Fig. 13. The effect of APC, with SM and DM references.

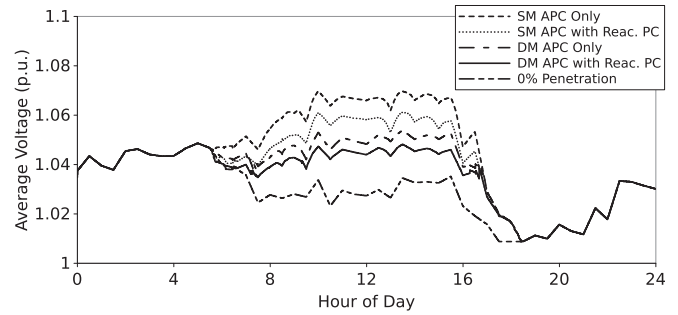


Fig. 14. Comparing APC-only against APC with reactive preferred, reactive power control (PC).

By implementing both the SM and DM type APC-only models, significant voltage reduction, as shown in Fig. 13, can be attained. It is clear that the DM APC-only model achieves much better voltage regulation than the SM APC-only model, reducing power based on the operating conditions at the time when the over-voltage condition occurred, rather than just having a fixed nominal response. The DM APC-only model reduces overvoltage by approximately 40–60% (of the voltage difference between the 100% penetration and 0% penetration cases), whereas the SM APC-only model reduces over-voltage by approximately 20–25%. When considering these and other results, note that the PV penetration levels being tested, and the nature of the (weak) grid modelled in this example were intentionally chosen to illustrate the performance of over-voltage mitigation strategies and should not be seen as typical of the prevalence of over-voltage conditions or the associated curtailment losses throughout actual distribution networks.

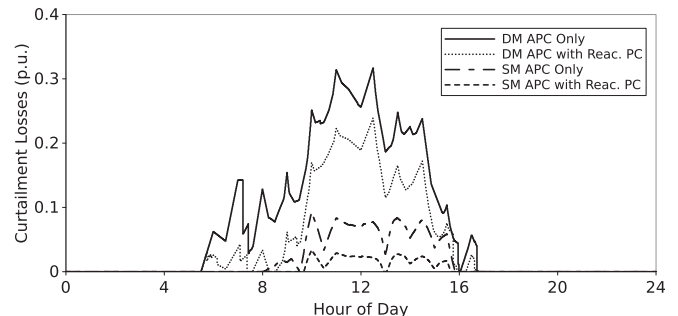


Fig. 15. Curtailment losses for the simulated control schemes.

Table 1
Comparison of the different control schemes at 12 noon.

Control method	Curtailement losses (p.u.)	Curtailement loss (relative)	Voltage @ 12:00 (p.u.)	Overvoltage reduction (%)
None – 100% penetration	0	N/A	1.0796	0%
SM, APC only	0.069	1.00	1.0659	26%
SM, APC with Reac. Pref	0.023	0.33	1.0581	41%
DM, APC only	0.256	3.71	1.0483	60%
DM, APC with Reac. Pref	0.189	2.74	1.0440	68%
None – 0% penetration	0	N/A	1.0274	100%

Further simulations were carried out to compare the effectiveness of the APC-only type models against models which also feature reactive power injection and absorption. A comparison of the resulting network voltage regulation performance is shown in Fig. 14. For this scenario, it is clear that the inclusion of reactive power control produces a significant improvement in over-voltage conditions, when compared to the equivalent APC-only strategies (i.e. comparing SM type against SM type and DM type against DM type). In this case, the inclusion of the reactive power preferred volt–var function has resulted in additional voltage reductions of around 15% and 8% for the SM and DM cases respectively.

More significantly, in all cases, the inclusion of the volt–var functionality is found to substantially reduce curtailment losses while simultaneously providing better voltage regulation. This is clearly shown in Fig. 15 and numerical results (for 12-noon, when PV power output is at its peak) are recorded in Table 1.

Although the specific performance obtained depends on the particular scenario, these results show that the use of volt–var in combination with volt–watt power quality functions provides improved voltage regulation and reduces curtailment losses. This will be of particular interest and benefit to PV generation system owners who would otherwise forego revenue at times when the network hosting capacity is exceeded. DM controls have been shown to provide better voltage regulation (than SM), though this is clearly at the expense of additional curtailment losses and additional control complexity. It is clear that the decision not only to include power quality management functions, but also which functions and how the interactions between them are managed will contribute significantly to the PV generation hosting capacity of distribution networks.

6. Conclusions

This paper evaluates the effectiveness of real and reactive power control, of distributed PV inverter systems, to manage network voltage rise problems while avoiding excessive curtailment of potential solar generation capacity. High resolution PV generation, customer load and network voltage data has been collected at a number of trial sites in Newcastle, Australia and forms the basis for simulation models used. Network impact simulations were undertaken on both a small example problem and for a long rural feeder from the Australian National Feeder Taxonomy Study.

For given nominal volt–var and volt–watt power quality functions, seven different implementations were described and investigated. These occur due to the use (or not) of the reactive power function and different treatments of the interaction of these power quality functions with the inverter apparent power limits and the choice of either referencing the response to the current operating conditions or to the inverter rating. Using these power quality management functions, PV inverters are able to regulate distribution network voltages and reduce network losses. The result of this is an increased network hosting capacity, facilitating the continued uptake of distributed renewable energy.

The results of this analysis show that:

- a control scheme that implements a dynamic-maximum type control scheme is more effective at reducing overvoltage compared to a static maximum type model, but this comes at the expense of greater curtailment losses;
- a control scheme that implements reactive power absorption reduces curtailment losses *whilst reducing overvoltage to a greater extent* (compared to an equivalent model without).

While the simulation studies in this paper focused on a MV long rural feeder, further research will investigate how this applies to other feeders within the Australian NTFS and hence the Australia-wide impact of such results. Furthermore, while this paper uses NTFS feeder models and experimentally obtained PV and load data for setting up the simulation system, it will be important to follow up this simulation work with an actual implementation of the schemes to verify their actual performance.

Acknowledgements

This paper was published as part of the Virtual Power Station 2 project. This project received funding from the Australian Renewable Energy Agency (ARENA) 2014/RND032. The views expressed herein are not necessarily the views of the Australian Government, and the Australian Government does not accept responsibility for any information or advice contained herein.

References

- [1] Sayeef S, Heslop S, Cornforth D, Moore T, Percy S, Ward JK, et al. Solar intermittency: Australia's clean energy challenge. Tech. Rep. CSIRO; 2012. <http://www.csiro.au/~media/CSIROau/Flagships/Energy%20Transformed%20Flagship/Solar%20intermittency/FINAL%20Solar%20intermittency%20Australias%20clean%20energy%20challenge.pdf>.
- [2] Schneider KP, Chen Y, Chassin DP, Pratt RG, Engel DW, Thompson SE. Modern grid initiative distribution taxonomy final report. Tech. Rep. PNNL-18035. Richland, WA (US): Pacific Northwest National Laboratory (PNNL); 2008.
- [3] Electric Power Research Institute (EPRI). Common functions for smart inverters. Version 3. Tech. Rep. 3002002233. Palo Alto, CA, USA: EPRI; 2013. <http://www.epri.com/abstracts/Pages/ProductAbstract.aspx?ProductId=00000000001026809>.
- [4] Tonkoski R, Lopes LAC, EL-Fouly THM. Coordinated active power curtailment of grid connected PV inverters for overvoltage prevention. IEEE Trans Sustain Energy 2011;2(2). ISSN: 1949-3029:139–47. <http://dx.doi.org/10.1109/TSTE.2010.2098483>.
- [5] Tonkoski R, Lopes LAC, EL-Fouly THM. Droop-based active power curtailment for overvoltage prevention in grid connected PV inverters. In: IEEE International Symposium on Industrial Electronics; 2010. p. 2388–93. <http://dx.doi.org/10.1109/ISIE.2010.5637511>.
- [6] Turitsyn K, Sulc P, Backhaus S, Chertkov M. Local control of reactive power by distributed photovoltaic generators. In: First IEEE International Conference on Smart Grid Communications; 2010. p. 79–84. <http://dx.doi.org/10.1109/SMARTGRID.2010.5622021>.
- [7] Smith J, Sunderman W, Dugan R, Seal B. Smart inverter volt/var control functions for high penetration of PV on distribution systems. In: IEEE/PES Power Systems Conference and Exposition; 2011. p. 1–6. <http://dx.doi.org/10.1109/PSCE.2011.5772598>.
- [8] Cagnano A, Torelli F, Alfonzetti F, De Tuglie E. Can PV plants provide a reactive power ancillary service? A treat offered by an on-line controller. Renew

- Energy 2011;36(3). ISSN: 0960-1481:1047–52. <http://dx.doi.org/10.1016/j.renene.2010.08.036>. <http://www.sciencedirect.com/science/article/pii/S0960148110004076>.
- [9] Liao Y, Fan W, Cramer A, Dolloff P, Fei Z, Qui M, et al. Voltage and var control to enable high penetration of distributed photovoltaic systems. In: North American Power Symposium; 2012. p. 1–6. <http://dx.doi.org/10.1109/NAPS.2012.6336328>.
- [10] Mohamed Y-R, El-Saadany E. Adaptive decentralized droop controller to preserve power sharing stability of paralleled inverters in distributed generation microgrids. *IEEE Trans Power Electron* 2008;23(6). ISSN: 0885-8993: 2806–16. <http://dx.doi.org/10.1109/TPEL.2008.2005100>.
- [11] Elexon. Load profiles and their use in electricity settlement. 2004. https://www.elexon.co.uk/wp-content/uploads/2013/11/load_profiles_v2.0_cgi.pdf.